Hydrogeochemical model of Debaga Basin, Northeast Iraq

Al-Tamimi, Omer Sabah[1]; Unger-Lindig, Yvonne[2]; Merkel, Broder[2]

[1] *Department of Applied Geology, Tikrit University Tikrit, Iraq omeribrahiem@yahoo.com*

[2] *Technische Universitaet Freiberg, Institut für Geologie, Gustav-Zeuner-Straße 12, 09596 Freiberg, Germany*

(**Received:** 10 / 4 / 2012 ---- **Accepted:** 8 / 5 / 2012)

Abstract

Hydrogeochemical characteristics of groundwater in Debaga Basin were studied. PhreeqC-modeling was done for 99 water analysis including calculation of Saturation Indices (SI) ,precipitation and dissolution of calcite and gypsum, respectively. Variations of the pore space resulting from the last two processes were also highlighted. Because of the fact that the groundwater is mainly used as irrigation water, processes which may influence the water chemistry were also modeled. These processes are equilibration with atmospheric conditions (degassing of CO_2) and losses of irrigation water by evaporation up to 20%. The groundwater in Debaga Basin is supersaturated with respect to calcite and dolomite and under-saturated with respect to gypsum. However, precipitation of calcite will have no negative influence on pore space. Changes in water chemistry will mainly occur by degassing of CO_2, which will result in a lower solubility for calcite and an increase of the SI for calcite. This significant super saturation with respect to calcite will lead to precipitation of calcite, since the water is used as irrigation water. This will mainly affect the calcite content of the agricultural soils, which are still shows high calcite concentrations. Evaporation losses of the irrigation water have only slightly influence on further precipitation of calcite.

Keywords: hydrochemical modeling, Debaga Basin, Iraq,

Introduction

The Debaga Basin is a well studied area in Northern Iraq. Numerous studies were of mainly geological interests (e.g. AL-SAMARIA 1977; AL-QALANCHI 1981; FUAAD 1983). The first geological investigations were performed by Turkish petroleum companies (e.g. CREEK & MASON 1926; LONG 1926; ANDRAU & HENSON 1928; BIRAUD 1928). MCFAYDEN (1935) investigated the water supply of the Basin and provided therefore the first hydrogeological informations about Debaga Basin. Further hydrogeological investigations were done by e.g. PARSONS (1955), MOHAMMAD (1981), AL-ANSARI et al. (1990), AL-TAMIMI (2002), AL-SUDANY (2003) and JAWAD (2002). JAWAD et al. (2007) evaluated the groundwater resources of Debaga Basin for utilization as irrigation water. BURINGH (1960) studied the soils in the Basin and in other areas in Iraq, whereas BELLEN (1956) investigated the limestone of Kirkuk and Bai Hassan Formations deposited in the basin.

The main aim of this study to establish a hydrochemical model for Debaga Basin focusing on saturation indices (SI) for different mineral phases (especially, gypsum, calcite and dolomite). Based on the modeled SI, influence on porosity of the aquifer was investigated caused by precipitation or dissolution processes. Thereby, the SI is defined as the logarithm of the quotient of the ionic activity product (IAP) and solubility product (SP) of a mineral phase.

$$SI = \log\left(\frac{IAP}{SP}\right) \quad \ldots\ldots\ldots\ldots\ldots (1)$$

The SI indicates if a solution is in equilibrium, super-saturated or under-saturated with respect to a mineral or a solid phase.

The groundwater in Debaga Basin is often used as irrigation water by sprinkler irrigation (JAWAD et al. 2007). It is well known, that in arid and semi arid areas like Debaga Basin irrigation may lead to salinization of groundwater and soil (e.g. OREN et al. 2004, YUE 2007; VALENZA et al. 2000, AL-TAMIMI 2002). Therefore, changes in water chemistry as a result of irrigation were also modeled for the groundwater in Debaga Basin.

The Debaga basin is located between 35° 30' 00" N, 43° 22' 30" E and 36° 07' 30" N, 44° 15' E in the north-east of Iraq (Figure 1). It is a high undulated terrain bounded by the Avana Mountains at the south-west and Qarachauq Mountains at north-east. The Upper and Lower Zab River (also called Greater and Lesser Zab) border the basin at the north-west and south-east boundary, respectively. The basin has a north-west to south-east orientated rectangular shape with a dimension of 18 times 75 km (nearly 1400 km^2). This orientation follows the general direction of the major folds in this area. The basin slopes from the central part towards both rivers. The altitude ranges between 330 m a.s.l. in the central part to 230 m a.s.l. at the banks rivers. The Avana and Qarachauq Mountains reach an altitude up to 500 and 870 m a.s.l., respectively. The plain is cut by a dendritic and parallel drainage pattern (AL-SAMARAI 1977). An elevated subsurface structure at the centre splits the drainage system into two systems (Kindawa and Kandinawa). The Kindawa catchment area is part of the Upper Zab River and the Kandinawa drains into the Lower Zab River (Figure 1).

Rainfall in Iraq shows a gradual increasing pattern to north eastern direction, following the rising topography. In the centre of Debaga Basin the annual average rainfall is about 375 mm (JAWAD et al. 2007). From long time records at the Kirkuk meteorological station (1980-2006), it is obvious that in the dry season, the real evaporation exceeds significantly the rainfall. In the middle of the wet season from December to February, the real evaporation and the rainfall are balanced (Figure 2). The Kirkuk

meteorological station is located about 70 km south-east of Debaga Basin.

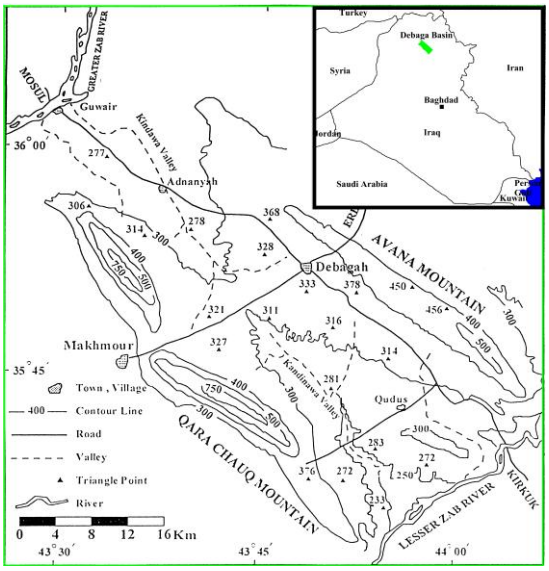

Figure 1: Location map of Debaga Basin (modified after AL-SUDANY 2003).

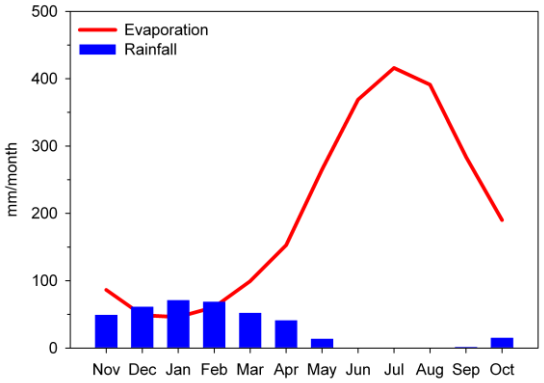

Figure 2: Monthly means of rainfall and evaporation at Kirkuk meteorological station.

Geology and Hydrogeology of Debaga Basin

The Debaga Basin is restricted by the two anticlines Qarachauq and Avana (also called Kirkuk structure). These anticlines are part of a northwest-southeast orientated parallel fold system. This fold zone is a result of plate tectonics involving the Arabian and Iranian plates during the alpine orogenesis (JASSIM & GOFF 2006).

The folded formations are cretaceous deposits and middle Eocene to Pliocene sediments. The cretaceous formations consist of marl, mudstone, and limestone with a thickness ranging from 60 and 150 m. The Eocene units represented by the Jadala and Avana formations are exposed only in the Qarachauq anticline. The sediments of the Jadala formation consists mainly of chert and chalky limestones with a thickness of about 45 m. The largest part of the Qarachauq anticline is exposed by formations of the Oligocene composed of limestone and dolomite. Outcrops of the Miocene sediments of the Fatha and Injana Formations can be found at both anticlines (Figure 3). The Fatha formation is widely exposed within the basin. It consists of cyclic deposits of marl, limestone, and gypsum. The Injana formation consists of grey and brown sandstone interbedded by brown clay stone and reddish brown siltstone. The thickness of this formation varies between 45 and 398 m. The Miocene-Pliocene Mukdadiya formation consists of coarse grained sandstones and soft clay stones. The thickness of this formation ranges between 40 and 456 m. The Pliocene sediments represented by the Bai Hassan Formation are composed of brown mudstone and coarse poorly consolidated conglomerates with a varying thickness of 30 to 2500 m. The Quaternary sediments can be divided into an older and younger alluvium. The older alluvium, which occurs in the plain, are heterogeneous deposits of lenticular and commonly elongated bodies of sand, clay, secondary gypsum, and poorly sorted gravels, mostly derived from topographic heights in the region. Younger alluvium however, is a flood plain stream deposit composed of gravel and sand with considerable silt and clay (BUDAY 1980, SISSAKIAN 1992).

Two types of soil are associated with weathering of the sediments of the Bai Hassan and Mukdadiya Formations. The first type is a reddish brown soil, which is composed of old river sediments covering calcareous layers. The dark brown soil is generated over limestone and gravel of the Bai Hassan and Mukdadiya Formations. This texture of the soil is silty clay to clay. Below the brown surface horizon, the colour turns to light grey, which indicates an accumulation of calcite (BURINGH 1960).

Groundwater bearing formations (Aquifers)

The upper most formations of the syncline starting with the recent and ending with the Upper Miocene contain beds that can be described as groundwater bearing horizons. The Quaternary deposits occur in two forms: river terraces at the vicinity of the main rivers, and the Pleistocene-Holocene sediments which cover most of the plain area. The river terraces are mainly composed of weak cemented gravels and therefore expected to be important aquifers. However, these deposits have very limited extents and a maximum thickness of 25 m. The Pleistocene-Holocene sediments are deposits of variable sources composed of silt, clay, sand, and some pebbles or gravels and form the shallow unconfined aquifer (JAWAD et al. 2007).

The Pleistocene-Holocene sediments are underlain by Pliocene conglomerates of the Bai Hassan formation. These conglomerates are considered as the most permeable formation of clastic sediments in Northern Iraq. However, the Bai Hassan formation has only limited thickness in Debaga Basin. Moreover the formation has important intercalations of sandstones and impermeable mudstone beds (JAWAD et al. 2007). The next groundwater bearing horizon in the sequence consists of Upper Miocene-Pliocene

sediments of the Mukdadiya formation. These sediments are composed of coarse sandstone and pebbly sandstone beds and impermeable mudstone horizons (JAWAD et al. 2007).

The fine sandstone beds of the Upper Miocene have the largest extent in the basin. Normally they occur at several horizons separated by impermeable beds of siltstone and clay which compose the Injana formation. More clay stone as well as gypsum beds are found with depth as the Middle Miocene Fatha formation encountered. The Injana formation has considerable thickness which has not been fully penetrated by the existing wells in the basin (JAWAD et al. 2007). Two types of aquifers are recognized in the basin, the shallow or unconfined aquifer consists of Quaternary sediments and the confined aquifer, which combines the permeable beds in the three tertiary formations Bai Hassan, Mukdadiya, and Injana. The separation between the two aquifer types is based on flow net type and the usual presence of an impermeable bed at the top of the Bai Hassan Formation (AL-TAMIMI 2002; AL-SUDANY 2003). The unconfined aquifer shows a variable saturated thickness, which does not exceed 25 m. It is tabbed by wells with a maximum depth of 70 m. The maximum thickness of the unconfined aquifer occurs in the centre of the southern and the northern sub basin. The confined aquifer varies in saturated thickness between 50 and 75 m. It is tabbed by wells with a depth between 90 and 250 m (JAWAD et al. 2007).

Groundwater flow in the unconfined aquifer follows the surface drainage pattern in the basin (Figure 4). Potential values of about 400 m occur at eastern and western boundaries and dropping in northern and southern directions to less than 200 m near the discharge zones at the two Zab Rivers. The flow converges towards two main valleys in the Basin. The groundwater in the confined aquifer however, follows the synclinal structure of the basin (Figure 5). The subsurface structure at the basin centre plays again, the role of a groundwater flow divide. From the centre the groundwater flows in opposite directions to the Upper and Lower Zab River, respectively (AL-TAMIMI 2002; JAWAD et al. 2007). Values of hydraulic properties were determined for the confined aquifer – the main aquifer – by previous studies (e.g. AL-TAMIMI 2002, AL-SUDANY 2003).

Transmissivities vary between 126 and 917 m²/d (median: 177 m²/d) in the former study. Those given by the later range between 65 and 2315 m²/d (median: 168 m²/d). The mean aquifer storage coefficient is stated with $6.6 \cdot 10^{-3}$ and $2.7 \cdot 10^{-3}$, respectively. Hydraulic properties for the unconfined aquifer are not available so far.

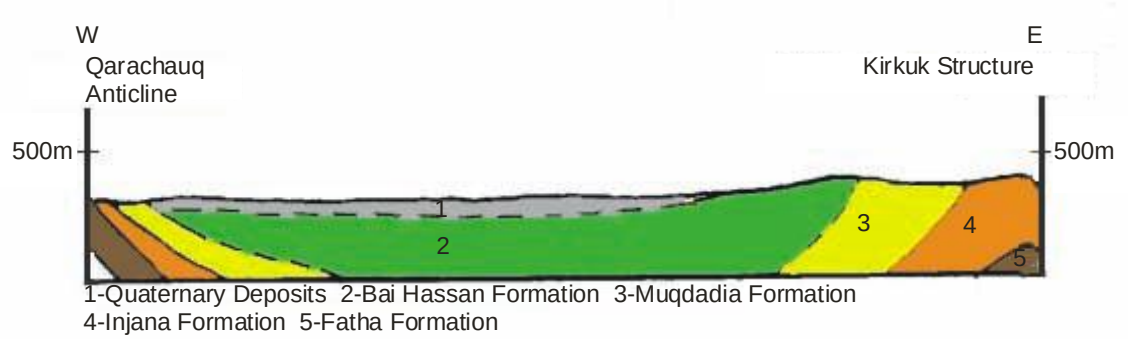

Figure 3: Geological cross section of Debaga Basin (after SISSAKIAN

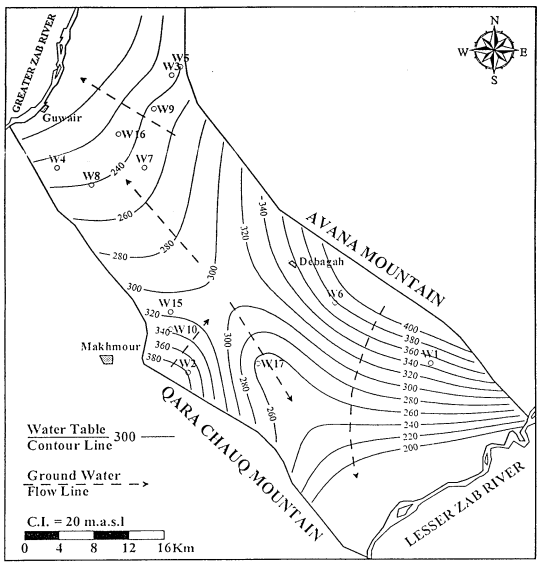

Figure 4: Groundwater flow pattern of the unconfined aquifer (AL-SUDANY 2003).

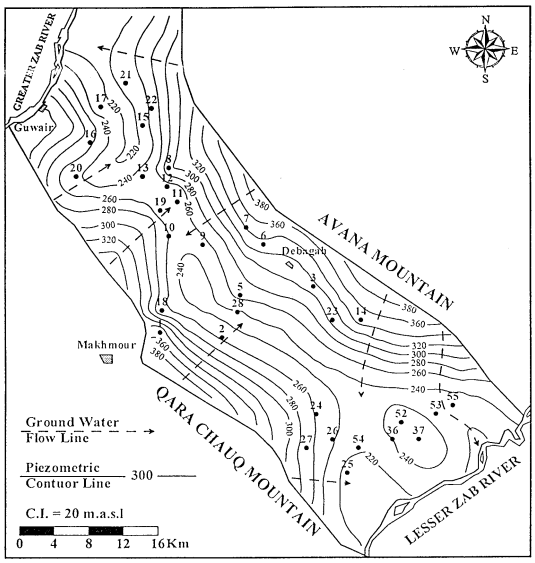

Figure 5: Groundwater flow pattern of the confined aquifer (AL-SUDANY 2003).

Material and Methods

Groundwater chemistry data were available from a survey in 2002 (AL-TAMIMI 2002) and data collected between 1965 and 1980 (hydrogeological database) from the Ministry of water resources/Iraq. (Appendix A). The wells from the 2002 survey can be divided into two groups. 29 wells penetrate the confined aquifer (deep wells) and 9 wells are located in the unconfined aquifer (shallow wells). Such a differentiation is not possible for the 61 wells of the hydrogeological database. A third data set from JAWAD et al. (2007) was also available. However, only three analyses of 19 had an error of analyze below 10%, thus this data set was neglected for the research.

In the 2002 survey Na and K were analyzed as sum parameter by flame photometer. Ca and Mg were determined by titration with EDTA using eriochrom black T and murexid as indicator. The anions Cl, SO_4 and NO_3 were analyzed by colorimetry. Bicarbonate and carbonate were determined by titration using methyl orange and phenolphtalein as indicator. The pH-value was measured with a pH-meter. Dry weight of water at 105 °C is equal to the total dissolved solids (TDS). All analyzes were done by (water and soil researches laboratories – Ministry of water resources – Iraq).

As first step of the hydrogeochemical modeling using PhreeqC (PARKHURST & APPELO 1999), the percent error for all analyzes was calculated by the following equation:

$$\frac{\left|\sum Cation - \sum Anion\right|}{\sum Cation + \sum Anion} \cdot 100\% = error \quad \ldots\ldots\ldots\ldots (2)$$

Thereby the cations and anions are used in equivalent concentrations. PhreeqC was used to calculate saturation indices (SI) and to model changes in groundwater chemistry, resulting from the utilization as irrigation water. The Wateq4F-database was used for all calculations. Na and K were measured as sum parameter in the 2002 survey. Comparison of the 2002 data with the data from the hydrolgeological database shows Na concentration equal to the sum of Na and K. Thus, the sum of Na and K was used as Na in the PhreeqC-modeling. The sum of bicarbonate and carbonate was defined as the concentration of HCO_3. In some analyzes, from the hydrogeological database of (ministry of water resources – Iraq) , no pH-value were measured. In these cases, the pH value was replaced by the mean value of all analyzes (7.9).

Results and Discussion

The absolute value of the error varies between 0.04% and 9.7% (mean: 2.4%) for the analyses of the 2002 survey and between 0.08% and 6.7% (mean: 2.2%) for the analyses from the hydrogeological database, respectively (Appendix A). However, three analyzes in the data from the hydrogeological database had an insufficient accuracy (No. 56: 48.2%, No 52. -14.7%, and No. 14: 18.5%). These analyses were excluded from the hydrogeochemical modeling.

The groundwater in the unconfined aquifer is supersaturated with respect to calcite and dolomite, and under-saturated regarding to gypsum (Table 1). The ionic activity product (IAP) is about 4.5 times higher than the solubility product (SP) for calcite and about 40 times higher for dolomite, respectively.

The distribution pattern of the SI for calcite and dolomite is quite similar (Figure 5a, 6a). In the middle of the basin toward to the north-east, the groundwater is slightly supersaturated with respect to calcite and dolomite. The SI for calcite is about 0.3 and for dolomite 0.6, which means that the groundwater is twofold supersaturated with respect to calcite and fourfold supersaturated with respect to dolomite. The SI increases for both minerals towards to the Upper and Lower Zab at the north-west and south-east boundary, respectively. The SI near the Zab Rivers is about 0.8 for calcite and 1.4 to 1.8 for

dolomite, therefore the IAP is six fold supersaturated and 25 to 50-fold supersaturated with respect to calcite and dolomite, respectively. This distribution pattern is equal to the groundwater flow pattern in the unconfined aquifer (Figure 3). However, it has to be considered that most of the shallow wells are located near the boundary of the basin. Thus, conclusions about the distribution pattern and the reasons for, in the unconfined aquifer are of lower significance.

On the opposite, the groundwater in the unconfined aquifer is under-saturated with respect to gypsum. However, the SI increases from the north-east part of the basin (SI=-1.4) towards to the Rivers Upper Zab and Lower Zab, respectively (Figure 7a). The distribution pattern of the SI for gypsum complies with the distribution pattern of the concentration of calcium (Figure 9a). Although, the sulphate concentration pattern (Figure 10a) looks quite different in the south-east part of the basin, the distribution pattern of the SI for gypsum and Ca concentration are an indication that gypsum, contained in the unconfined aquifer, is dissolved in the groundwater. The difference between sulphate and calcium, especially in the lower basin, is caused by the few numbers of wells in this area.

The SI of the minerals calcite, dolomite, and gypsum as well as the pCO_2 seems to be more even in the shallow wells than in the deeper wells (s. below). However, this may be only the result of the lower number of wells compared to deeper wells.

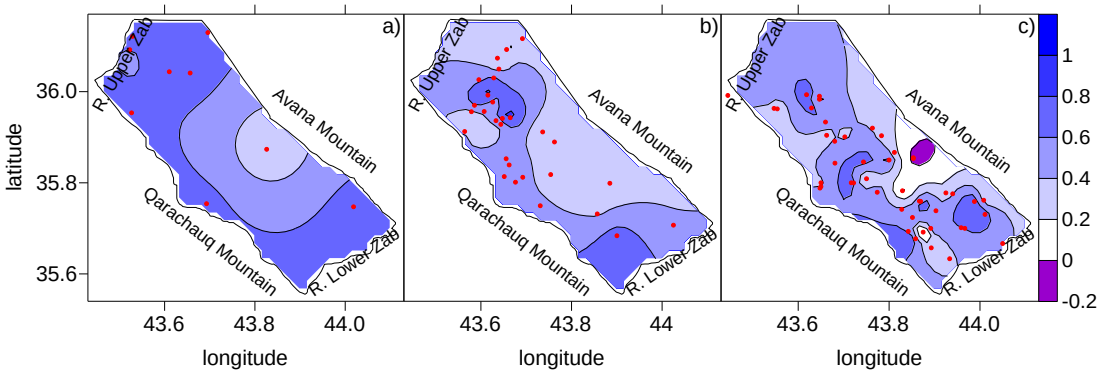

Figure 5: Distribution of the SI for calcite a) shallow wells; b) deep wells; c) wells of the hydrogeological database (red points = sample points).

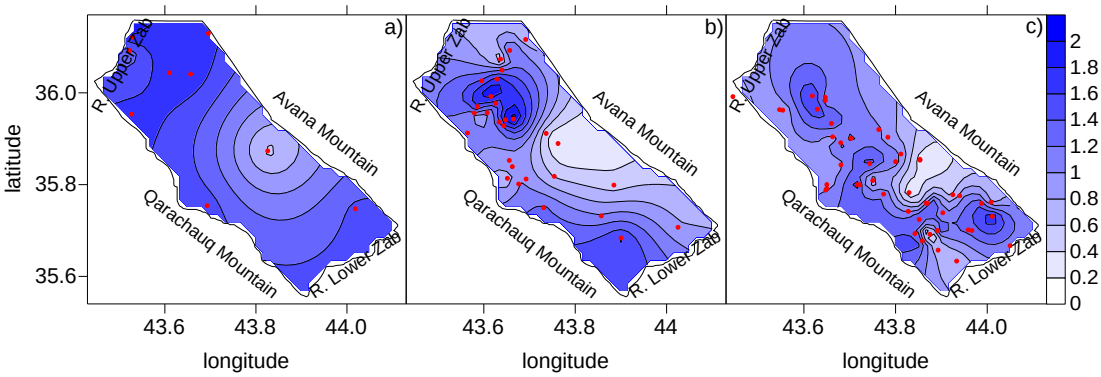

Figure 6: Distribution of the SI for dolomite a) shallow wells; b) deep wells; c) wells of the hydrogeological database (red points = sample points).

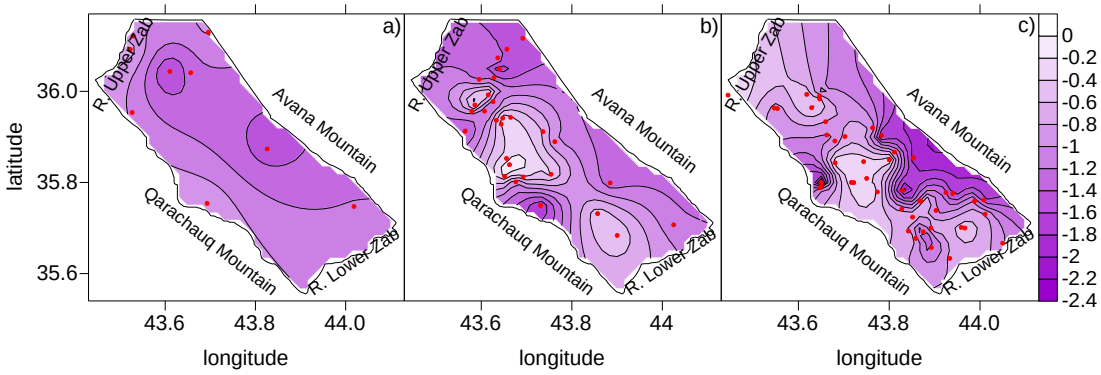

Figure 7: Distribution of the SI for gypsum a) shallow wells; b) deep wells; c) wells of the hydrogeological database (red points = sample points).

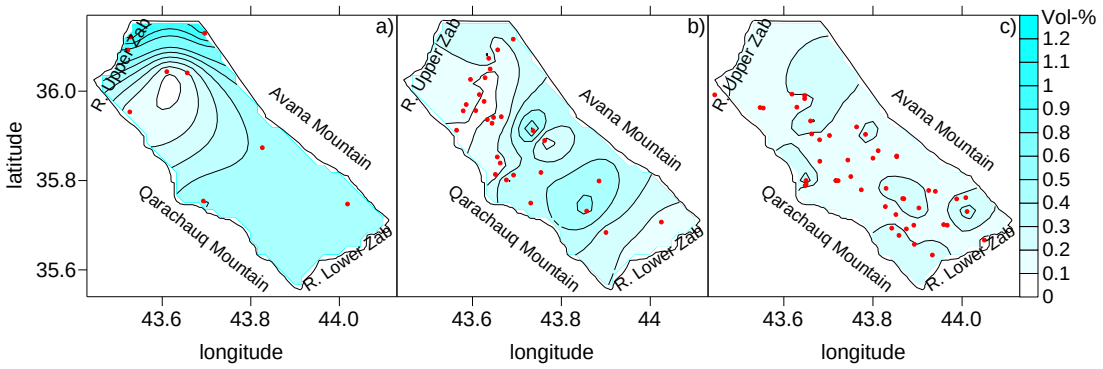

Figure 8: Distribution of the pCO_2 a) shallow wells; b) deep wells; c) wells of the hydrogeological database (red points = sample points).

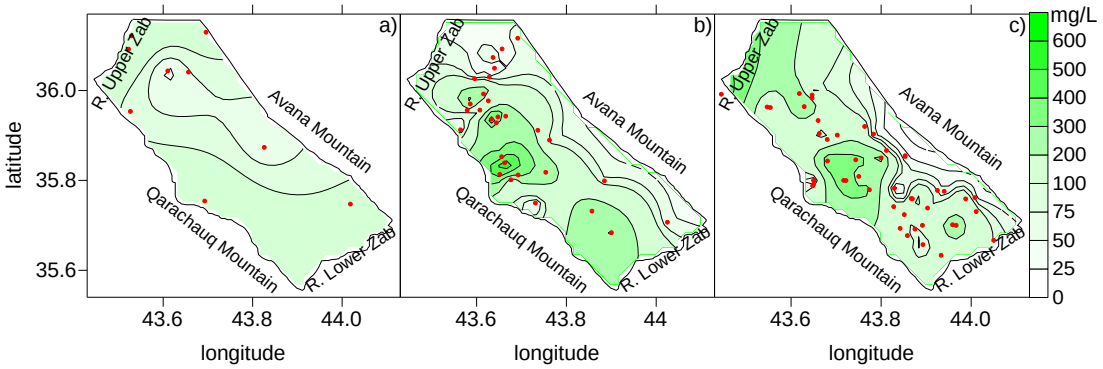

Figure 9: Distribution of Ca concentration a) shallow wells; b) deep wells; c) wells of the hydrogeological database (red points = sample points).

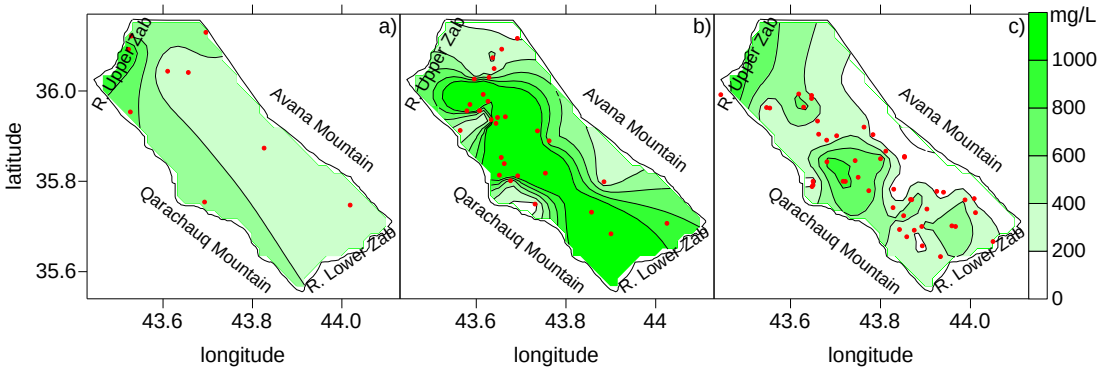

Figure 10: Distribution of SO_4 concentration a) shallow wells; b) deep wells; c) wells of the hydrogeological database (red points = sample points).

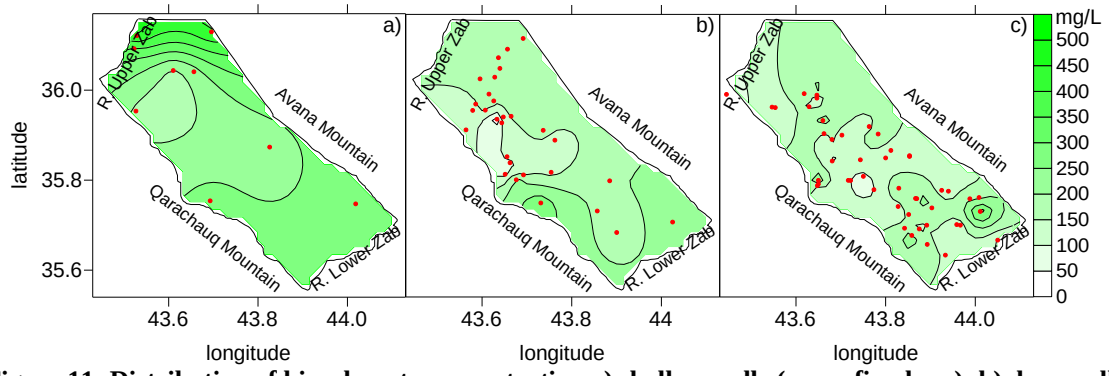

Figure 11: Distribution of bicarbonate concentration a) shallow wells (unconfined aq.); b) deep wells (confined aq.); c) wells of the hydrogeological database (red points = sample points)

Table 1: Mean (Min, Max) values for Saturation Index for calcite, dolomite, and gypsum and related interesting parameters.

	Investigation from 2002 (AL-TAMIMI 2002)		**hydrogeological**
	deep wells (>150 m)	**shallow wells**	**database**
Ca (mg/L)	200.9 (24-634)	109.5 (40-166)	162.3 (17-491)
HCO3 (mg/L)	155.2 (2-284)	291.6 (189-455)	151.1 (71-336)
SO_4 (mg/L)	1160 (102-3400)	480 (192-1030)	389.8 (40.8-1180)
SI calcite	0.47 (0.16-0.89)	0.62 (0.21-0.75)	0.43 (-0.43-0.84)
SI dolomite	1.12 (0.2-2.12)	1.49 (0.53-1.82)	1.01 (-0.29-1.79)
SI gypsum	-0.86 (-1.83-0.06)	-1.12 (-1.68- -0.67)	-0.92 (-2.27- -0.04)
pCO2 (Vol.-%)	0.22 (0.08-0.65)	0.51 (0.09-1.05)	0.18 (0.07-0.38)
electrical conductivity (µS/cm)	3330 (710-7800 (11500))	1730 (780-2700)	2002 (280-8000)

The groundwater in the confined aquifer is under-saturated, with respect to gypsum and supersaturated with respect to calcite and dolomite (Table 1). The IAP for calcite is about 2.8 times higher than the SP (median: 2.5) and for dolomite about 19.6 (median: 8.3), respectively. The SI for dolomite varies more in the different wells, than for calcite. The IAP for gypsum is only 30% (median: 10%) of the SP.

The spatial pattern of the SI for calcite and for dolomite in the deep wells follows nearly the flow pattern of the unconfined aquifer in the northern part (Figure 5b, 6b). However, the SI for calcite and dolomite are lower than in the unconfined aquifer. The lowest SI for calcite and dolomite (SI=0.2-0.4) are in the centre part of the basin, with an increase towards the Upper and Lower Zab River. In contrast to the unconfined aquifer, the maximum is not at the Zab Rivers, but in the centre part of the north-west part of the basin.

Resulting from the spatial pattern of the SI for calcite and dolomite and the super-saturation of the groundwater, with respect to calcite, it is most likely that calcite originates from the unsaturated zone or from the unconfined aquifer. Calcite dissolution will be enhanced by high partial pressure of CO_2 (pCO_2) (STUMM & MORGAN 1996). In the deeper wells (< 150 m) the pCO_2 is below 0.5 Vol.-% (Figure 8b), however, in the soil pCO_2 may reach values up to 100x atmospheric levels, caused by microbiological activity and respiration of plant roots (BERTHELIN 1988). The water of the confined aquifer is in equilibrium with calcite, if the pCO_2 is higher than in the solution (up to 1.3 Vol.-%). Thus, the super-saturation of calcite in the confined aquifer as well as the high calcite concentrations in the soil indicates that calcite is dissolved in the unsaturated zone, caused by higher pCO_2 in the soil. In deeper zones of the aquifer (<100 m) far below the vegetation level, the pCO_2 decreases resulting in a super-saturation of calcite.

On the opposite the SI for gypsum decreases from the inner part of the basin (SI=0 to -0.2) to northeast and southwest (SI=-1.4 to 1.6), respectively. As can be seen in Figure 7b this spatial pattern is more consistent with the flow pattern of the groundwater in the confined aquifer. This distribution pattern of the SI for gypsum indicates that gypsum is dissolved in the confined aquifer and not in the infiltrating zone. The infiltrating water is under-saturated with respect to gypsum, but in flow direction in the confined aquifer dissolution of gypsum occurs. The distribution of concentration of Ca and SO_4 shows the same pattern like the SI for gypsum (Figure. 9b, 10b). Increased concentrations of these both elements can be found in the inner part of the basin as a result of dissolution of gypsum. On contrary to the bicarbonate concentration, which is higher in the unconfined aquifer, the SO_4 concentration in the unconfined aquifer is lower than in the confined (Figure 10 a, b; 11 a, b). This is a further indication that gypsum is dissolved mainly in the confined aquifer.

Influence on porosity

Due to the super-saturation of calcite, it is possible that calcite may precipitate in the aquifer. In the unconfined aquifer a maximum of about 80 mg calcite may precipitate from one Liter of groundwater. Assuming a density of 2.65 g/cm³ for calcite, this is about 0.03 cm³. Caused by the lower super-saturation in the confined aquifer, a maximum of 30 mg (0.01 cm³) calcite may precipitate from one Liter of groundwater (Table 2). These values are so low that they will not impact the pore space significantly. Furthermore, the assemblage of dissolved gypsum exceeds the calcite precipitation, thus, decreasing of pore space by the precipitation of calcite can be neglected. On the other hand, extension of the pore space by dissolution of gypsum is also marginal. If we assume a groundwater volume (Q) of 35 L/d (k_f: $1.875 \cdot 10^{-7}$ m/s; n_e: 0.2), which enters a groundwater body of 1m³, and gypsum will be dissolved until reaching equilibrium (SI=0), this extension will be not more than 40 cm³/d and 15 dm³/y, respectively.

Table 2: Assemblage of calcite precipitation and gypsum dissolution.

well	$CaCO_3$ precipitation (mg/L)	$CaCO_3$ precipitation (cm^3/L)	$CaSO_4$ dissolution (mg/L)	$CaSO_4$ dissolution (cm^3/L)
deep wells (confined aquifer)				
1	7.78	0.003	670.2	0.29
2	12.24	0.005	283.0	0.12
3	11.82	0.004	1271.2	0.55
4	23.40	0.009	686.3	0.30
5	7.59	0.003	1286.1	0.56
7	6.56	0.002	2498.0	1.09
8	8.28	0.003	2386.7	1.04
9	4.75	0.002	2165.2	0.94
10	5.09	0.002	2149.0	0.93
11	19.91	0.008	878.0	0.38
12	8.41	0.003	2409.5	1.05
13	29.50	0.011	907.1	0.39
14	25.25	0.010	1220.8	0.53
15	8.10	0.003	2525.2	1.10
16	5.62	0.002	2589.2	1.13
17	11.09	0.004	2440.2	1.06
18	15.22	0.006	2410.9	1.05
19	7.38	0.003	2313.7	1.01
20	7.15	0.003	1820.6	0.79
21	8.95	0.003	2523.2	1.10
22	8.83	0.003	2466.5	1.07
23	6.49	0.002	1262.3	0.55
24	17.50	0.007	1294.3	0.56
25	23.60	0.009	2325.8	1.01
26	17.97	0.007	2654.9	1.15
27	11.68	0.004	2287.7	0.99
28	26.97	0.010	1554.1	0.68
29	17.85	0.007	1585.6	0.69
shallow wells (unconfined aquifer)				
30	18.27	0.007	2291.3	1.00
31	24.22	0.009	2459.4	1.07
32	14.73	0.006	2599.8	1.13
33	43.64	0.016	1892.3	0.82
34	79.44	0.030	2335.4	1.02
35	7.31	0.003	2557.1	1.11
36	41.67	0.016	2117.2	0.92
37	37.58	0.014	2408.7	1.05
38	69.84	0.026	2350.7	1.02

Evaporation during irrigation

Besides the problem that the SI of calcite and dolomite will increase, as a result of the CO_2 degassing, increasing SI will occur, when the irrigation water partly evaporates. This process was also modeled with PhreeqC. In the first step of modeling the water was partly removed. The remaining solution has the same chemical composition but in less solvent, thus the solution will be enriched. Various authors propose an evaporation loss for sprinkler irrigation of up to 20 % (e.g. FROST & SCHWALEN 1955, MARTINEZ-COB et al. 2008,

PLAYAN et al. 2005, YAZAR 1984). Therefore, different rates of evaporation (5, 10, 15, and 20%) were modeled. The SI for calcite in the water from the deep wells ranges between 1.2 and 1.3 with an evaporation rate of 5 and 20%, respectively (Table 3). Comparing to the values in equilibrium with atmosphere, the SI for calcite as well as dolomite increases only slightly by evaporation.

The SI of gypsum varies between -0.77 (evaporation 5%) to -0.67 (evaporation rate 20%) in deep wells and -1.1 to -1.0 in shallow wells, respectively. Although the SI for gypsum increases slightly, gypsum is still under-saturated and will not precipitate. Thus, the gypsum content of the groundwater shows no limitations for using groundwater as irrigation water.

Table 3: Mean Saturation Index for a modelled evaporation of 5 and 20 % of irrigation water.

	deep	shallow
SI calcite (5%)	1.18	1.52
SI calcite (20%)	1.27	1.61
SI dolomite (5%)	2.54	3.30
SI dolomite (20%)	2.71	3.47
SI gypsum (5%)	-0.77	-1.11
SI gypsum (20%)	-0.67	-1.01

Variations of the Saturation Index with time

Variations of the hydrogeochemistry in the groundwater of Debaga Basin may be evaluated by comparing the data from the 2002 survey with the hydrogeological database between 1965 and 1980. The SI for calcite ranges from 0.2 to 0.9 in the 2002 survey and -0.4 to 0.8 in the data from the hydrogeological database, respectively (Table 1). The groundwater in the older data is slightly under-saturated with respect to calcite in the north-east part of the basin. An increasing of the SI of calcite can also be found at the southern boundary near the Lower Zab River (Figure 5). However, in other parts of the basin (i.e. near the Upper Zab River, south-west part of the basin) the SI for calcite decreased or is at least in the same range comparing with deeper wells. Comparison of the database wells with the shallow wells of the 2002 survey shows a significant increase of the SI for calcite in all parts of the basin.

The SI for dolomite varies between 0.2 and 2.1 in the wells of the 2002 survey and between -0.3 and 1.8 in the wells of the hydrogeological database. As well as calcite, the SI for dolomite increases in all parts of the basin comparing the wells in the unconfined aquifer (2002 survey) and hydrogeological database (Figure 6). However, the confined aquifer shows again both increasing (near the southern boundary, northern subbasin) and decreasing SI values for dolomite (north east boundary).

References

AL-ANSARI, N., JASSIM, M.D., ABASS, H.A., SARKISS, H.K. (1990): Economic and Strategic Importance of groundwater in Iraq. Technical Report, 30 p.

AL-QALANCHI, J.S. (1981): Gravitational geophysical investigation on gypsum rocks that suitable for the manufacture of plaster building, Makhmour District-Erbil Governorate. Library of general institute of minerals, Baghdad, 145 p.

AL-SAMARAI, A. (1977): Regional geological mapping of Makhmour-Kirkuk area. Technical report, Library of S.O.M., Baghdad.

AL-SUDANY H.I. (2003): Hydrogeological System of Debaga Basin in North of Iraq. Ph.D Thesis , University of Baghdad ; 153 p .

AL-TAMIMI, O.S. (2002): Evaluation of Groundwater in Debaga Basin /North East Iraq. MSc Thesis, University of Baghdad 95 p.

ANDRAU, E.W.K., HENSON, F.R.S. (1928): Geology report on Qara chaugh Dagh structure. - I.N.O.C. Library, No.GR 37, Baghdad, Iraq.

BELLEN, R.C. (1956): The stratigraphy of the main limestone of the kirkuk, Bai Hassan, Qara chaugh Dagh structures. Inst.-Petroleum Journal 42 (393), 233-263.

BERTHELIN, J. (1988): Microbial weathering processes in natural environments. In: LERMAN, A., MEYBECK, M. (eds.): Physical and chemical weathering in geochemical cycles. Kluwer, Dordrecht, pp 33-59.

BIRAUD, F. (1928): Geology report on Qara chaugh dagh structure. I.N.O.C. library No. 38, 39p.

BUDAY, T. (1980): The Regional Geology of Iraq .Vol .1 , Stratigraphy and Palaeogeography. Publication of GEOSURV, Baghdad , 445 p.

BURINGH, P. (1960): Soils and Soil Condition in Iraq. Ministry of Agriculture, Baghdad.

CREEK, C.W., MASON, S.L. (1926): Report on the Regional Geology east of Tigris between Lesser Zab to Qara Chaugh Dagh. - I.N.O.C. Library, No. GR. 13, Baghdad. Iraq.

FROST, K.R., SCHWALEN, H.C. (1955): Sprinkler evaporation losses. Agric. Eng. 36 (8), 526-528.

FUAAD, S.F. (1983): Structural and geological study to quaterny folds. MSc. Thesis, College of Sciences-University of Baghdad, 201 p.

JASSIM, S.Z., GOFF, J.C. (2006): Geology of Iraq. – Brno, Dolin Hlavni, 241 p.

JAWAD, A.M. (2002): Hydrogeological studies and investigation of Block 9-Daibaga and Makhmour areas. Technical report, Ministry of Irrigation, Baghdad-Iraq, 61 p.

JAWAD, S. B., MOHAMMAD, I. J., JAWAD, A. M., KADHIM, K. J., GATEE, H. H. (2007): Groundwater Irrigated Agriculture Management in the Daibaga Hydrogeological Basin (North East Iraq). Report Arab Science & Technology Foundation, 65 p.

Long, H.K. (1926): The Bai Hassan-Juraji Structure and Kirkuk Structure and Qwair Structure. - I.P.C. Report, I.N.O.C. Library No. GR 18, Baghdad.

MARTINEZ-COB, A., PLAYAN, E., ZAPATA, N., CAVERO, J., MEDINA, E.T., PUIG, M. (2008): Contribution of Evapotranspiration Reduction during Sprinkler Irrigation to Application Efficiency. Journ. of Irrigation and Drainage Engineering 134 (6), 745-756.

MCFAYDEN, W.A. (1935): Water supply in Iraq. Water supply paper 12, 2-5.

MOHAMMAD, K.M. (1981): Hydrogeological study to Greater Zab Basin in Iraq. MSc. Thesis, College of Art-University of Baghdad, 200 p.

OREN, O., YECHIELI, Y., BOEHLKE, J.K., DODY, A. (2004): Contamination of groundwater under cultivated fields in an arid environment, central Arava Valley, Israel. Journal of Hydrology 290 (3-4), 312-328.

PARKHURST D. L., APPELO C. A. J. (1999): User`s guide to PHREEQC (Version 2): a computer program for speciation, batch reaction, one-dimensional transport, and inverse geochemical calculations. - US Geological Survey, Water Resources Investigations Report 99-4259, p. 312.

Parsons, R.M. (1955): Groundwater Resources of Iraq. Vol. 5, Erbil Liwa, S.O.M. Library, Baghdad-Iraq,

Playan, E., Salvador, R., Faci, J.M., Zapata, N., Martinez-Cob, A., Sanchez, I. (2005): Day and night wind drift and evaporation losses in sprinkler solid-sets and moving laterals. Agricultural Water Management 76 (3), 139-159.

Sissakian, V.K. (1992): The Geology of Kirkuk Quadrangle. Dept. of geological survey, NI-38-2, 48 p.

Stumm W., Morgan J. J. (1996): Aquatic Chemistry. - New York et al.: John Wiley & Sons, 1022 p.

Valenza, A., Grillot, J.C., Dazy, J. (2000): Influence of groundwater on the degradation of irrigated soil s in a semi-arid region, the inner delta of the Niger River, Mali. Hydrogeology Journal 8 (4), 417-429.

Yazar, A. (1984): Evaporation and drift losses from sprinkler irrigation systems under various operating conditions. Agricultural Water Management 8 (4), 439-449.

Yue, W. Yang, J. Tong, J. Gao, Z. (2007): Analysis of water and salt balance in a semi-arid irrigation district (China) – A case study. Water-Rock Interaction 1-2,

الموديل الهيدروجيوكيميائي لحوض ديبكة شمال شرق العراق

عمر صباح ابراهيم التميمي[1] ، ايفون لندنك[2] ، برودير ميركل[2]

[1] *كلية العلوم ، جامعة كركوك ، كركوك ، العراق*

[2] *جامعة فريبيرك التكنولوجية ، جمهورية المانيا الاتحادية*

(تاريخ الاستلام: 10 / 4 / 2012 ---- **تاريخ القبول:** 8 / 5 / 2012)

الملخص

تم في هذا البحث دراسة الخصائص الهيدروجيوكيميائية للمياه الجوفية في حوض ديبكة الواقع شمال شرق العراق باستخدام برنامج (Phreeq C) المصمم لنمذجة حالة تفاعل ماء صخر. حيث جرى تقييم الحوض باعتماد (99) نموذج مائي من جوانب دلائل الاشباع (SI) ، كمية الترسيب والذوبان لمعدني الكالسايت والجبسم والتركيز على تغايرحجم الفراغات الناجمة عن العمليتين المذكورتين اعلاه ، كون ان الاستخدام الرئيسي للمياه الجوفية في هذا الحوض هو لاغراض الري بالتالي توجب التعرف على حالة الذوبان والترسيب وتوازن كل منهما مع الظروف الجوية (ذوبان غاز CO_2) وفقدان جزء من مياه الري عن طريق عملية التبخر الذي يشكل 20% من حجم الضائعات ، وقد توصل الى ان المياه الجوفية في هذا الحوض هي بحالة فوق الاشباع بالنسبة لمعدني الكالسايت و الدولومايت وتحت الاشباع بالنسبة لمعدن الجبسم ، عندها يكون لمعدن الكالسايت تاثيراً على حجم الفراغات داخل الوسط المسامي وان التغييرات الكيميائية للمياه تتاثر بشكل رئيسي بذوبان غاز CO_2 والذي يؤدي الى تقليل ذوبانية الكالسايت وزيادة الـ (SI) له والذي يكون كافيا بدوره لحدوث عملية ترسيب معدن الكالسايت وبسبب استخدام مياه الحوض الجوفية (المورد المائي الرئيسي في الحوض) لاغراض الري ادى الى التاثير في نوعية تربة الحوض ، حيث زادت نسبة تركيز معدن الكالسايت فضلا عن تاثير الضائعات الناجمة عن تبخر المياه والتي بدا تاثيرها اقل في عملية الترسيب هذه.